



## Original Article

## The role of natural rock filler in optimizing the radiation protection capacity of the intermediate-level radioactive waste containers

O.L. Tashlykov<sup>a</sup>, M.S. Alqahtani<sup>b, c</sup>, K.A. Mahmoud<sup>a, d, \*</sup><sup>a</sup> Ural Federal university, 19 Mira St, Yekaterinburg, 620002, Russia<sup>b</sup> Department of Radiological Sciences, College of Applied Medical Sciences, King Khalid University, Abha, 61421, Saudi Arabia<sup>c</sup> Bioluminescence Unit, Space Research Centre, Department of Physics and Astronomy, University of Leicester, Leicester, LE1 7RH, United Kingdom<sup>d</sup> Nuclear Materials Authority, P.O. Box 530, El-Maadi, Cairo, Egypt

## ARTICLE INFO

## Article history:

Received 12 March 2022

Received in revised form

26 April 2022

Accepted 14 May 2022

Available online 17 May 2022

## Keywords:

Radioactive waste containers

Equivalent dose rate

Monte Carlo simulation

Natural rocks

## ABSTRACT

The present work aims to optimize the radiation protection efficiency for ion-selective containers used in the liquid treatment for the nuclear power plant (NPP) cooling cycle. Some naturally occurring rocks were examined as filler materials to reduce absorbed dose and equivalent dose received from the radioactive waste container. Thus, the absorbed dose and equivalent dose were simulated at a distance of 1 m from the surface of the radioactive waste container using the Monte Carlo simulation. Both absorbed dose and equivalent dose rate are reduced by raising the filler thickness. The total absorbed dose is reduced from  $7.66E-20$  to  $1.03E-20$  Gy, and the equivalent dose is rate reduced from 183.81 to  $24.63 \mu\text{Sv/h}$ , raising the filler thickness between 0 and 17 cm, respectively. Also, the filler type significantly affects the equivalent dose rate, where the recorded equivalent dose rates are 24.63, 24.08, 27.63, 33.80, and  $36.08 \mu\text{Sv/h}$  for natural rocks basalt-1, basalt-2, basalt-sill, limestone, and rhyolite, respectively. The mentioned results show that the natural rocks, especially a thicker thickness (i.e., 17 cm thickness) of natural rocks basalt-1 and basalt-2, significantly reduce the gamma emissions from the radioactive wastes inside the modified container. Moreover, using an outer cementation concrete wall of 15 cm causes an additional decrease in the equivalent dose rate received from the container where the equivalent dose rate dropped to  $6.63 \mu\text{Sv/h}$ .

© 2022 Korean Nuclear Society, Published by Elsevier Korea LLC. This is an open access article under the CC BY-NC-ND license (<http://creativecommons.org/licenses/by-nc-nd/4.0/>).

## 1. Introduction

Due to the expansion in the nuclear power plant (NPP) constructions, large volumes of radioactive wastes are produced each year during the operation process of these NPP [1]. The radioactive wastes released from the NPP are classified into three main classifications according to their level of activity concentrations, High (HLW), intermediate (ILW), and Low (LLW) [2,3]. These wastes are presented in various forms, solid, liquid, and gaseous states.

The HLW produced by the NPP industry is relatively small compared to the ILW and LLW wastes. The IAEA announced that around 392000 tons of heavy metal (tHM) have been discharged in the form of used fuel since the first NPP operation [4]. The LLW has a radioactive concentration of less than 4 GBq/ton for alpha

emission and less than 12 GBq/ton for beta emission. The transpose and handling of this type of radioactive waste don't require specific shielding material. The LLW represents around 90% of all radioactivity by volume and is mainly produced from hospitals and industry. On the other hand, the ILW represents 4% of all radioactivity by volume [4]. Its radioactivity level is higher than the LLW, thus, shielding materials are required during the handling and transposing of this type of radioactivity.

In order to treat the liquid radioactive wastes (LRW) and gaseous radioactive wastes (GRW), the particulate solids and aerosols should be separated first. In the case of LRW generated by the NPP, containers filled with ion-selective sorbent are used to separate the radioactive isotopes from the liquid. Ion-selective is one of the techniques used for the purification of the water cycle in the NPP [5]. Previous experimental showed that sorbent application is an effective technology for removing cesium and cobalt radioactive ions from LRW without preliminary ionization carried out at the NPP [6]. Thus, the sorbent inside the radioactive container was loaded by radioisotopes  $^{137}\text{Cs}$ ,  $^{134}\text{Cs}$ ,  $^{140}\text{Cs}$ ,  $^{90}\text{Sr}$ , and  $^{60}\text{Co}$  [6–10].

\* Corresponding author. Nuclear Materials Authority, P.O. Box 530 El-Maadi, Cairo, Egypt.

E-mail address: [karembdelazeem@yahoo.com](mailto:karembdelazeem@yahoo.com) (K.A. Mahmoud).

The mentioned radioisotope release almost all of the activity and equivalent dose rate in the area surrounding the hosting containers. Therefore, containers with high gamma-ray shielding capacity should be used in the NPP's liquid treatment to provide a safe place for workers with a permissible level of radioactivity not exceeds than 38  $\mu\text{Sv/h}$  [7,8,10–12]. In general, the total cost of managing, treating, and disposing of NPP's waste is very high, accounting for about 5% of the total cost of electric power generation [13].

Recently, many publications report high shielding properties for some natural occurring rocks. These publications concluded that the natural rock with high density such as basalt, gabbro, granite, charnockite, gneiss, magnetite, and hematite [14–19] have a suitable gamma ray shielding capacity to be used in the gamma-ray shielding applications.

The present work's novelty is to use the cheap widespread natural rock samples to reduce the equivalent dose rate from these liquid treatment containers. The container was modified by some natural rocks as fillers such as basalt-1, basalt-2, basalt-sill, limestone, and rhyolite. The Monte Carlo simulation code was utilized to detect the absorbed dose (D, Gy) and the equivalent dose rate (H,  $\mu\text{Sv/h}$ ) at 1 m from the surface of the modified container.

## 2. Materials and methods

The present work aims to modify a radioactive wastes container used in the ion-selective absorption process in the NPP to the treatment of the NPP cooling water and absorb the resident ions such as  $^{137}\text{Cs}$  and  $^{60}\text{Co}$  [8,9] with high activities reaches  $7.4\text{E}+11$  Bq. The current modification was performed by using the cheap and widespread natural rocks such as basalt-1, basalt-2, basalt-sill, limestone, and rhyolite as a filler material in the evacuated part separated the hosting capsule alloy made of (80 wt % of Pb+20 wt % of Zn) and the outer cementation concrete, as illustrated in Fig. 1. The chemical composition and density of the filler rocks were illustrated in Table 1. The effect of rock type and the rock thickness on optimizing the shielding properties of the container is studied using the Monte Carlo simulation method [20]. The radioactive waste container is assumed to be a cube in the shape with outer dimensions of  $162 \times 162 \times 121$  cm, as introduced to the input file. The container contains an inner cylindrical capsule with a height of 49.9 cm and a radius of 49 cm filled totally with the ion-selective resin loaded by the radioactive residues  $^{137}\text{Cs}$  and  $^{60}\text{Co}$ . In the present study, the tally F6 is used to evaluate the detector's absorbed dose per unit cell of the detector. The absorbed dose by the gamma photons emitted from the radioactive waste was

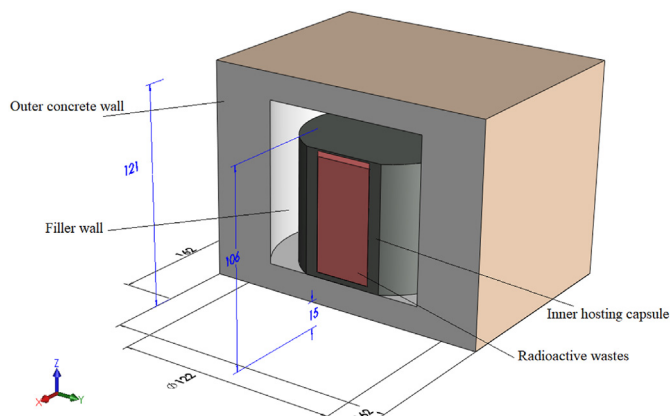


Fig. 1. The 3D-representation for Monte Carlo simulation input file for the radioactive waste container.

Table 1

The elemental chemical composition and density of the filler rocks used to modify the radioactive waste container.

Element	Chemical composition (wt.%)				
	limestone	basalt-sill	basalt-1	basalt-2	rhyolite
Al	0.46	5.57	5.42	5.52	0.29
O	48.94	29.74	30.43	30.48	23.79
Si	18.62	42.77	39.69	38.65	64.35
P	0.19	0.23	0.24	0.23	0.05
Ca	12.50	6.63	6.97	6.60	0.85
Mg	1.85	3.93	3.85	3.88	0.59
K	0.07	1.15	1.10	1.06	0.08
Na	0.98	1.62	2.81	2.86	0.12
Fe	3.63	7.13	7.76	7.89	8.68
Mn	0.02	0.15	0.19	0.15	0.01
Ti	0.42	0.65	0.97	0.97	0.00
H	0.12	0.27	0.30	0.37	0.08
Density ( $\text{g}/\text{cm}^3$ )	2.44	2.68	2.93	2.93	2.42

recorded on a detector cell placed at 100 cm from the surface of the container. For accurate determination of the absorbed dose, six detector cells were used (one detector in front of each face of the container), then the average absorbed dose was calculated. The absorbed dose in the detector cells was recorded. After that, the equivalent dose rate raised from the direct exposure to the container was calculated.

## 3. Results and discussion

### 3.1. Effect of filler thickness

The effect of the intermediate layer on the fabricated container's protection capacity was studied. The basic concept of the present studied stage is that the container consists of the inner capsule with 3 cm of PZ1 alloy. After that, the effect of filler thickness on the average absorbed dose was studied in Fig. 2, where the highest average absorbed dose is  $7.66\text{E}-20$  Gy. It is achieved for a 3 cm PZ1 capsule without filler material. After that, the filler thickness increases between 3 and 17 cm was associated with significant decreases in the absorbed dose recorded by detectors. For example, the average absorbed dose decreases in the order between  $4.50\text{E}-$

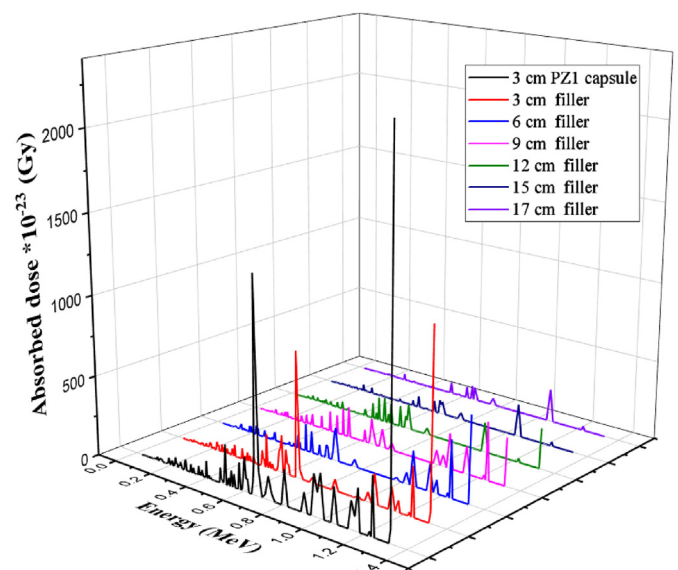


Fig. 2. Variation of the absorbed dose as a function of the filler thickness.

20, 3.43E-20, 2.52E-20, 1.62E-20, 1.17E-20, and 1.03E-20 Gy with raising the filler thickness between 3, 6, 9, 12, 15, and 17 cm, respectively. The recorded decrease in the average absorbed dose inside the filler layer is slighter than that recorded for the alloy capsule. This is attributed to the difference in the material characteristics used in the inner capsule and the filler layer. In the inner capsule, high dense alloy materials were used to overstand the corrosion and absorb the maximum number of photons emitted by the radioactive wastes due to the high photon absorption cross-section for the dense and high atomic number elements (Pb, Sn, W, and Bi) constituting the inner container. On the other hand, the intermediate filler layer consists of large thicknesses of widespread non-expensive materials with relatively low density compared to the inner capsule materials. A comparison between the absorbed dose recorded by the six detectors and the average absorbed dose were presented in Fig. 2. The mentioned figure illustrated that the dose rate recorded by all six detector are relatively close with a small differences between them as presented in Fig. 3.

The reduction in the absorbed dose mentioned early with increasing the filler thickness was reflected on the equivalent dose calculated for the detector cell. Fig. 4 illustrates that the equivalent dose decreases exponentially with raising the filler thickness. For example, the equivalent dose rate was reduced between 183.81, 108.10, 82.24, 60.48, 38.77, 28.05, and 24.63  $\mu\text{Sv/h}$  with growing the filler thickness between 0, 3, 6, 9, 12, 15, and 17 cm, respectively. The increase in the filler layer thickness means an increase in the track length of the photon transmitted from the PZ1 alloy capsule. The increase in the gamma photon's track length is associated with an increase in the collisions number between the photons transmitted from the PZ1 alloy capsule and the filler materials atoms. The interaction between photons and filler atoms depended on the activity of the radioactive wastes as well as the filler material characteristics (density and chemical composition). Thus, the photon transmitted from the PZ1 alloy capsule suffered more loss in their energy due to this interaction with the filler atoms. The net result is a decrease in the total number of photons transmitted from the container with 3 cm of PZ1 alloy's capsule+17 cm of the filler material.

The TF and RSC values' variation in the filler material was studied versus the filler thickness, as presented in Fig. 5. The TF

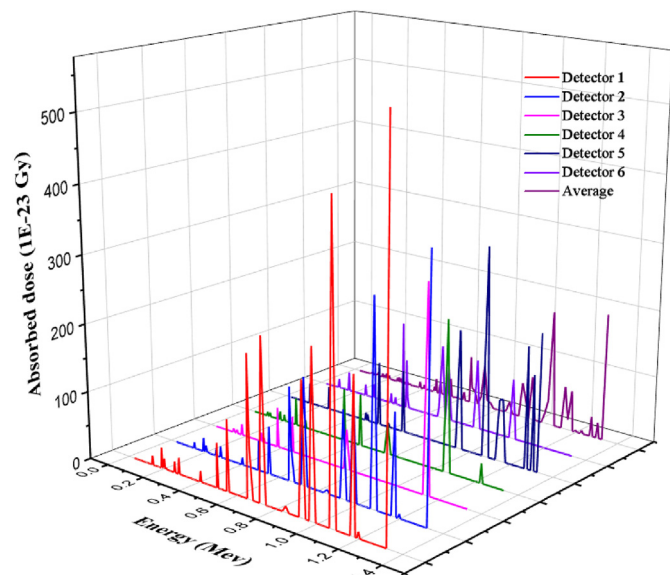


Fig. 3. Comparison between the absorbed dose recorded by the six detectors and the average absorbed dose.

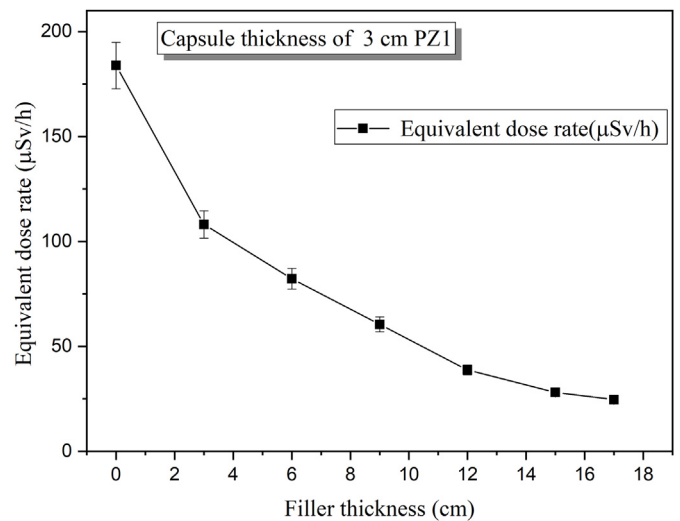


Fig. 4. Variation of the equivalent dose rate received versus the filler thickness (cm).

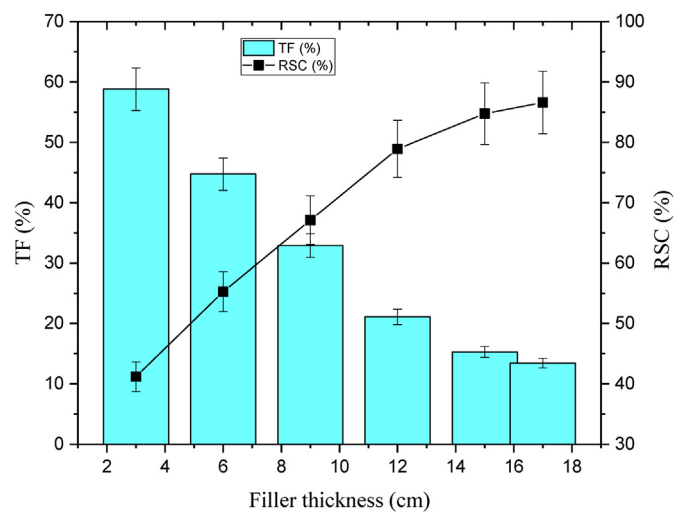


Fig. 5. Variation of both transmission factor and radiation shielding capacity versus the filler concentration.

values decrease between 58.81, 44.74, 32.90, 21.09, 15.26, and 13.40%, while the RSC increases from 41.19, 55.26, 67.10, 78.91, 84.74, and 86.60% with raising the filler thickness between 3, 6, 9, 12, 15, and 17 cm, respectively. As mentioned early, increasing the filler thickness causes an increase in the track length of gamma photons. This causes an increase in the amount of energy deposited inside the filler thickness by the collided photons. As a result, the number of photons that enable to penetrate the filler layer decreased, accompanied by a significant decrease in the number of photons reaching the detector. This means that the TF values decreases, and the RSC of the investigated container increases.

### 3.2. Effect of filler type

In this section, many natural rocks (basalt-1, basalt-2, basalt-sill, limestone, and rhyolite) with densities varied between 2.00 to 3.00  $\text{g/cm}^3$  were used fillers. The effect of these natural rocks in attenuation of the photon flux emitted from the PZ1 alloy's capsule was evaluated. Fig. 6 shows the variation of the absorbed dose (Gy) versus the filler types. The lowest average absorbed dose is

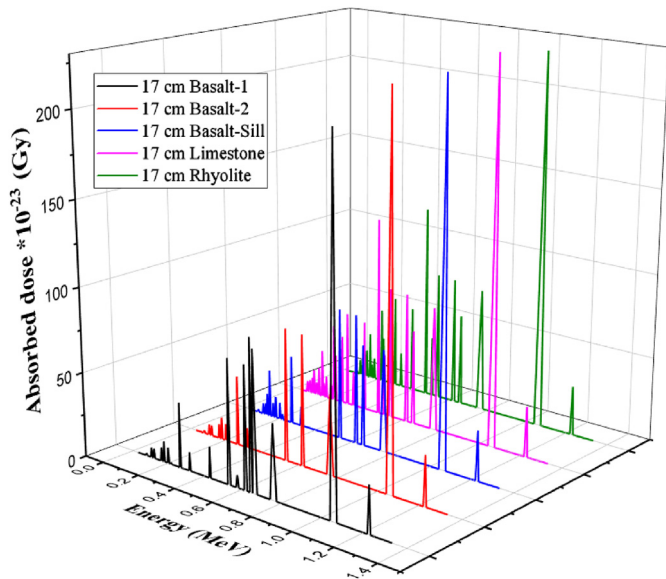


Fig. 6. The absorbed dose of the various filler rocks at various gamma-ray energies.

recorded for the fillers with a thickness of 17 cm from basalt-1 and basalt-2. The average absorbed dose is  $1.026E-20$  and  $1.003E-20$  Gy for filler materials basalt-1 and basalt-2, respectively. This low recorded average absorbed dose is due to the high density of the basalt samples basalt-1 and basalt-2 compared to other natural rocks used as a filler. Furthermore, the high content of Fe presented in these samples, where the Fe contents are 7.76 and 7.89 wt% for basalt-1 and basalt-2, respectively. In contrast, the sample rhyolite, which consists mainly of silica  $SiO_2$ , has the lowest density and the highest absorbed dose among the studied rock samples. The average absorbed dose for the rhyolite sample is  $1.503E-20$  Gy.

The equivalent dose reaches the detector was calculated when the radioactive wastes shield by 3 cm of the PZ1 alloy capsule and a thickness of 17 cm from the filler materials, as presented in Fig. 6. In this stage, it is observed that the highest equivalent dose rate of  $36.08 \mu Sv/h$  was recorded when the filler thickness was rhyolite rocks rich in  $SiO_2$ . In contrast, the lowest equivalent dose rates are  $24.07$  and  $24.63 \mu Sv/h$  received from the filler wall made of basalt-2 and basalt-1, respectively. Also, the equivalent dose rate received

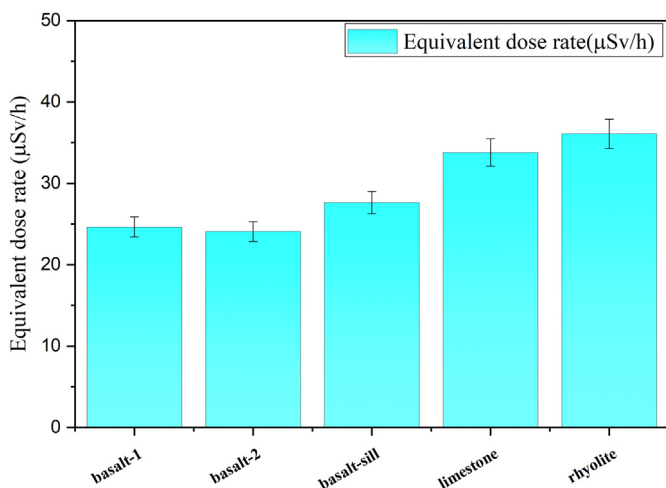


Fig. 7. The effect of various filler materials in the equivalent dose rate recorded by the detectors.

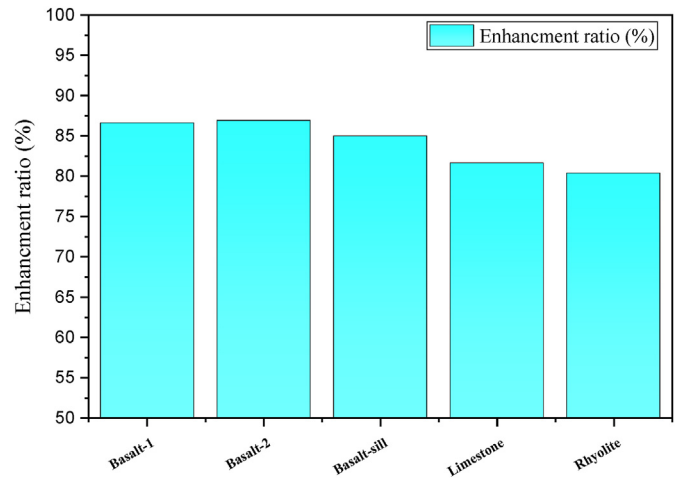


Fig. 8. The enhancement ratio in the shielding capacity of the container for various filler types.

from containers made of basalt-sill and limestone are  $27.63$  and  $33.80 \mu Sv/h$ .

As mentioned in Figs. 6 and 7, the equivalent dose rate and absorbed dose were varied with the material type used as filler. Thus, the shielding capacity enhancement ratio of the modified container was studied as a function of the material used. Fig. 8 showed that the best enhancement in the shielding behavior of the container was received when using a 17 cm thickness of basalt-1 and basalt-2 with enhancement ratios of 86.59 and 86.90%, respectively. This ratio was reduced to 84.97, 81.61, and 80.37% when the filler wall was made of basalt-sill, limestone, and -rhyolite, respectively. The calculation of this ratio is based on the number of photons incident on the filler wall thickness only (i.e., the number of photons that penetrate the PZ1 capsule and incident on the filler wall).

The absorbed dose in the detector cell at a distance of 100 cm from the surface of the container consists of three layers: 3 cm PZ1 shell capsule, 17 cm basalt-2 filler, and 15 cm M500 concrete, as shown in Fig. 9. As a result, the total amount of absorbed dose is significantly reduced from  $1.29E-18$  Gy to  $1.33E-21$  Gy for

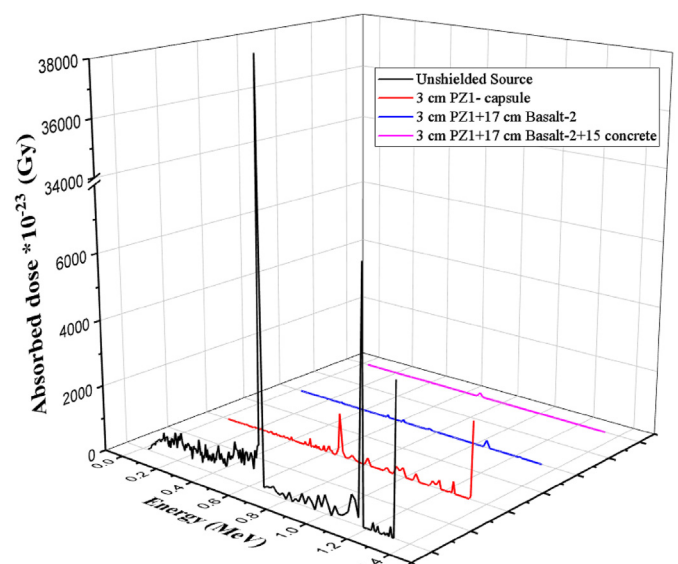


Fig. 9. Comparison between the absorbed dose recorded in each wall of the container.



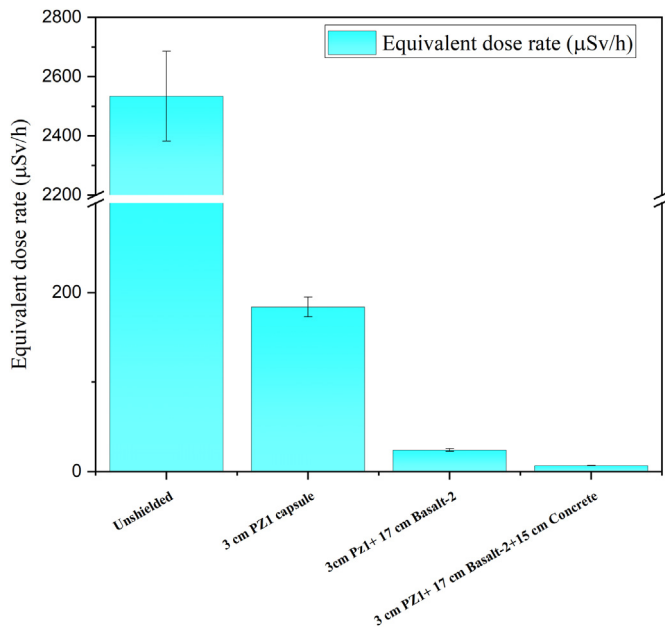


Fig. 10. Comparison between the recorded equivalent dose rate (µSv/h) for various walls consisting of the modified container.

unshielded radioactive material and when using three layers of container (3 cm thick PZ1, 17 cm thick basalt-2 filler, and external concrete 15 cm M500.

Based on the input energy recorded by the detectors, the equivalent dose rate received by the detector cell is calculated, as shown in Fig. 10. It is clear that the equivalent dose rate is reduced by 2534.03, 183.81, 24.1, and 6.63 µSv/h for unshielded radioactive waste, the container wall consists of hosting capsule with 3 cm of PZ1, the container wall of hosting capsule with 3 cm thickness of PZ1 + 17 cm thickness of filler basalt-2, and the container wall of hosting capsule of 3 cm thickness from PZ1 + 17 cm of the thickness of basalt-2+15 cm of concrete, respectively. As shown in Fig. 11, these results show that the hosting capsule thickness of 3 cm PZ1

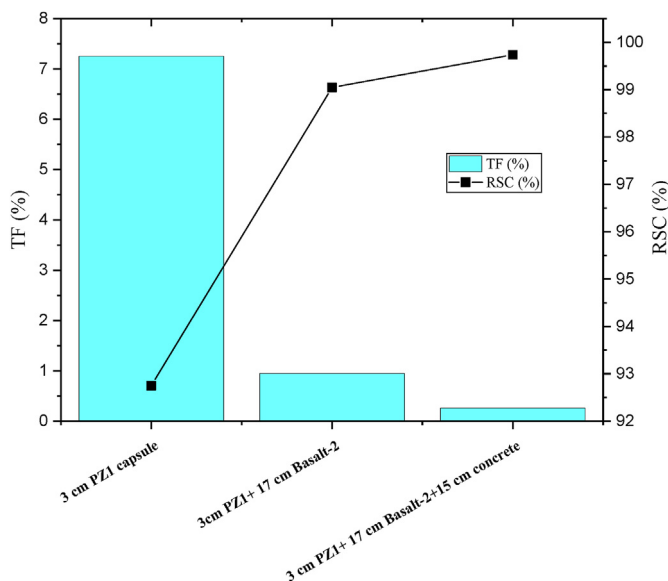


Fig. 11. The transmission factor and the radiation shielding capacity for each part of the modified container.

can stop about 92.75% of an emission activity, while a ratio of 7.25% can only penetrate the capsule thickness. Moreover, the addition of 17 cm of basalt-2 filler in the presence of the hosting capsule can stop almost all emitted photons (about 99.05% stopped), while only 0.95% penetrated through the thickness of the filler.

#### 4. Conclusion

The radiation protection efficiency of the radioactive waste container used for the treatment of the NPP cooling water was enhanced by using various natural rocks as a filler. In the present study, the effect of the filler thickness as well as the filler type on the radiation protection efficiency was evaluated. Using the Monte Carlo simulation, the obtained results illustrate that increasing the filler thickness causes a significant decrease in the absorbed dose and equivalent dose received at 1 m from the outer container wall surface. This study concluded that the recorded total absorbed dose is 7.66E-20 Gy from a hosting capsule with 3 cm thickness and chemical composition of 80 wt% Pb +20 wt% Zn. This mentioned absorbed dose is reduced to 4.50E-20, 3.43E-20, 2.52E-20, 1.62E-20, 1.17E-20, and 1.03E-20 Gy, raising the filler thickness between 3, 6, 9, 12, 15, and 17 cm, respectively. The illustrated reduction affected the equivalent dose recorded at 1 m from the container surface where the equivalent dose rate reduced exponentially from 183.81, 108.10, 82.24, 60.48, 38.77, 28.05, and 24.63 µSv/h, raising the filler thickness between 3 and 17 cm, respectively. Moreover, the study showed that the rock samples basalt-1 and basalt-2 were able to offer the highest safety level (have the lowest absorbed dose and equivalent dose rate) compared to other studied rock samples. The RPC for the optimized container increased from 41.19 to 86.59%, while the TF values decreased from 58.80 to 13.40%, raising the filler thickness between 3 and 17 cm, respectively. Finally, according to the mentioned results proofed by the Monte Carlo simulation, the natural non-expensive, widespread rocks can be helpful to reduce and optimize the shielding capacity for the radioactive waste containers used in the NPP.

#### Declaration of competing interest

The authors declare that they have no known competing financial interests or personal relationships that could have appeared to influence the work reported in this paper.

#### Acknowledgment

The authors extend their appreciation to the Deanship of Scientific Research at King Khalid University (KKU) for funding this research through the Research Group Program under the Grant Number : R.G.P.2/248/43.

#### References

- [1] S.H. Shin, W.N. Choi, S. Yoon, U.J. Lee, H.M. Park, S.H. Park, Y.J. Kim, H.R. Kim, Radiological analysis of transport and storage container for very low-level liquid radioactive waste, Nucl. Eng. Technol. 53 (2021) 4137–4141, <https://doi.org/10.1016/j.net.2021.06.024>.
- [2] International Atomic Energy Agency, Classification of Radioactive Waste, IAEA Safety Standards Series No. GSG-1, 2009.
- [3] J.N. Eiras, C. Payan, S. Rakotonarivo, V. Garnier, Experimental modal analysis and finite element model updating for structural health monitoring of reinforced concrete radioactive waste packages, Construct. Build. Mater. 180 (2018) 531–543, <https://doi.org/10.1016/j.conbuildmat.2018.06.004>.
- [4] International Atomic Energy Agency, Status and Trends in Spent Fuel and Radioactive Waste Management Series No. NW-T-1.14 (Rev. 1), 2022.
- [5] International Atomic Energy Agency, Processing of Nuclear Power Plant Waste Streams Containing Boric Acid, 1996.
- [6] V. Povarov, I. Gusev, S. Rosnovsky, D. Statsura, V. Kazansky, E. Goncharov, E. Mel'nikov, A. Volkov, S. Bulka, E. Ivanov, I. Korneev, Experience in implementation of systems applied for drainage water ion-selective purification

- from radionuclides at units 1,2 of Novovoronezh-2 NPP, ANRI (2020) 64–70, <https://doi.org/10.37414/2075-1338-2020-103-4-64-70>.
- [7] O.L. Tashlykov, Personnel Dose Costs in the Nuclear Industry. Analysis. Ways to Decrease. Optimization, LAP LAMBERT Academic Publishing GmbH & Co, RG, Saarbrücken, 2011.
- [8] Y.A. Kropachev, O.L. Tashlykov, S.E. Shcheklein, Optimization of radiation protection at the NPP unit decommissioning stage, *Izvestiya Vysshikh Uchebnykh Zawedeniy, Yadernaya Energetika.* (2019) 119–130, <https://doi.org/10.26583/npe.2019.1.11>, 2019.
- [9] O.L. Tashlykov, A.P. Khomyakov, S.v. Mordanov, V.P. Remez, in: Ion-selective Treatment as a Method for Increasing the Efficiency of Liquid Radioactive Waste Reducing in Accordance with Acceptance Criteria for Disposal, 2021, p. 20032, <https://doi.org/10.1063/5.0068413>.
- [10] G.A. Novikov, O.L. Tashlykov, S.E. Shcheklein, in: *Ensuring Safety in the Field of Nuclear Energy Use*, Ural State University Publ, Ekaterinburg, 2017.
- [11] A.F. Mikhailova, O.L. Tashlykov, The ways of implementation of the optimization principle in the personnel radiological protection, *Phys. Atom. Nucl.* 83 (2020) 1718–1726, <https://doi.org/10.1134/S1063778820100154>.
- [12] O.L. Tashlykov, Personnel Dose Costs in the Nuclear Industry. Analysis. Ways to Decrease. Optimization, LAP LAMBERT Academic Publishing GmbH & Co, RG, Saarbrücken, 2011.
- [13] International Atomic Energy Agency, Classification of Radioactive Waste A Safety Guide, 1994. <http://www-ns.iaea.org/standards/>.
- [14] N.K. Libeesh, K.A. Naseer, K.A. Mahmoud, M.I. Sayyed, S. Arivazhagan, M.S. Alqahtani, E.S. Yousef, M.U. Khandaker, Applicability of the multispectral remote sensing on determining the natural rock complexes distribution and their evaluability on the radiation protection applications, *Radiat. Phys. Chem.* 193 (2022), 110004, <https://doi.org/10.1016/j.radphyschem.2022.110004>.
- [15] N.K. Libeesh, K.A. Naseer, S. Arivazhagan, K.A. Mahmoud, M.I. Sayyed, M.S. Alqahtani, E.S. Yousef, Multispectral remote sensing for determination the Ultra-mafic complexes distribution and their applications in reducing the equivalent dose from the radioactive wastes, *The European Physical Journal Plus* 137 (2022) 267, <https://doi.org/10.1140/epjp/s13360-022-02473-5>.
- [16] S. Arivazhagan, K.A. Naseer, K.A. Mahmoud, K.V. Arun Kumar, N.K. Libeesh, M.I. Sayyed, M.S. Alqahtani, E.S. Yousef, M.U. Khandaker, Gamma-ray protection capacity evaluation and satellite data based mapping for the limestone, charnockite, and gneiss rocks in the Sirugudi taluk of the Dindigul district, India, *Radiat. Phys. Chem.* 196 (2022), 110108, <https://doi.org/10.1016/j.radphyschem.2022.110108>.
- [17] B. Mavi, Experimental investigation of  $\gamma$ -ray attenuation coefficients for granites, *Ann. Nucl. Energy* 44 (2012) 22–25, <https://doi.org/10.1016/j.anucene.2012.01.009>.
- [18] R.A.R. Bantan, M.I. Sayyed, K.A. Mahmoud, Y. Al-Hadeethi, Application of experimental measurements, Monte Carlo simulation and theoretical calculation to estimate the gamma ray shielding capacity of various natural rocks, *Prog. Nucl. Energy* 126 (2020), 103405, <https://doi.org/10.1016/j.pnucene.2020.103405>.
- [19] K.A. Mahmoud, O.L. Tashlykov, A.F. El Wakil, H.M.H. Zakaly, I.E. El Aassy, Investigation of radiation shielding properties for some building materials reinforced by basalt powder, *AIP Conf. Proc.* 2174 (2019), 020036, <https://doi.org/10.1063/1.5134187>.
- [20] X-5 Monte Carlo Team, MCNP — A General Monte Carlo N-Particle Transport Code, Version 5, La-Ur-03-1987. II, 2003.